

5. SYSTEM IMPLEMENTATION DOCUMENTATION

This section details the implementation phase of the previously presented designs, including experimental validation, model development, error correction, and the generation of manufacturing documentation (schematics, PCB layout, and bill of materials) for each subsystem.

5.1. Battery System and BMS Implementation

CELL TEST

The purpose of the cell test was to validate operation at higher charge currents in order to increase regenerative braking capability and improve overall pack performance. By confirming that the selected cell chemistry can safely accept higher C-rates, the HV battery can operate closer to its thermal and electrical limits, allowing greater energy recovery and efficiency during endurance driving.

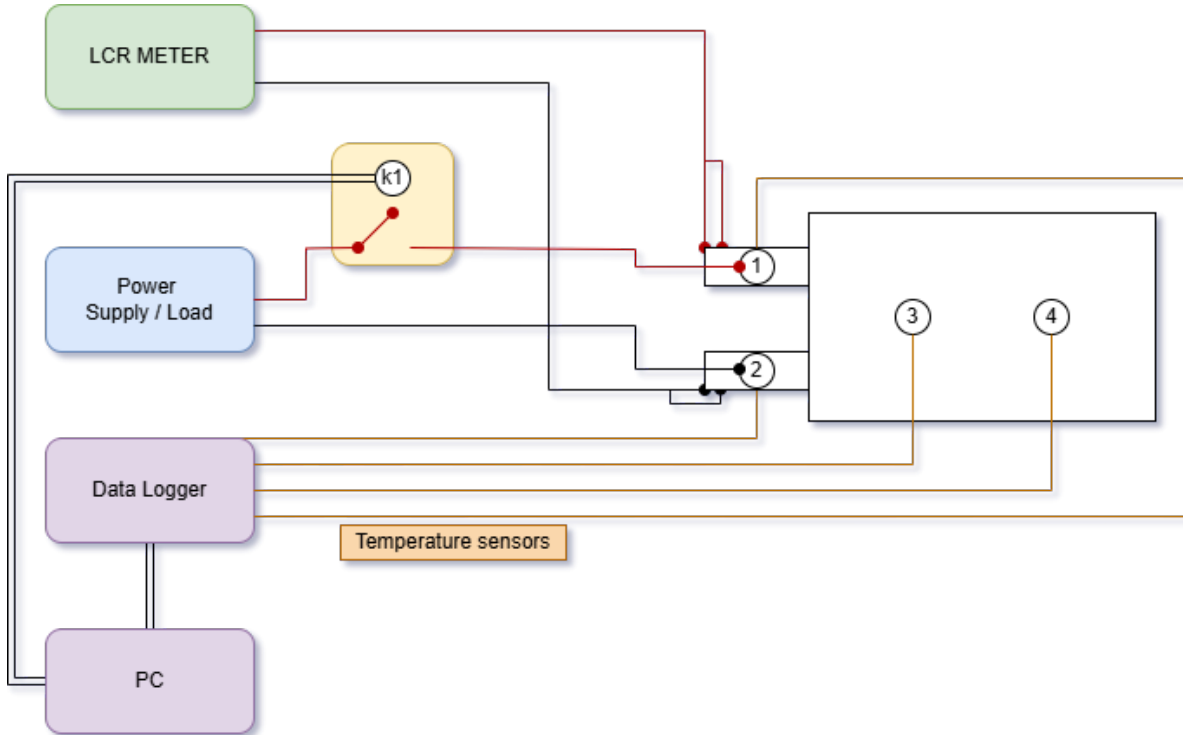


Image 8. Schematic of cell

Testing was conducted at Premium, a leading Catalan power electronics company, using industrial high-current power supplies not typically available in standard laboratory environments. The cell manufacturer required a minimum measurement resolution of 10 mV to validate current profiles and track cell voltage across all 50 cycles, including internal resistance values before and after each charge and discharge phase. An initial attempt to estimate internal resistance using a development board from the university electronics department proved unsuccessful. Multiple trials indicated that the measurement was operating at the noise threshold, since the cell resistance was expected to remain below 2 mΩ. Further analysis suggested that the excitation current used for resistance

calculation was too high, pushing the cell into a non-linear region and causing instability in the measurement.

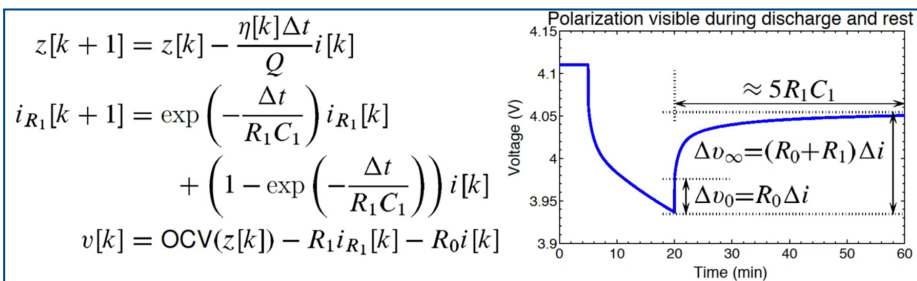
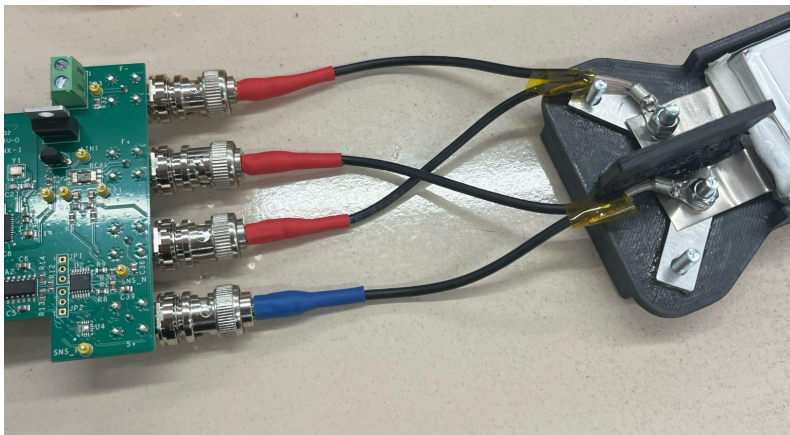


Image 9. Testing of cell

For this reason, at Premium we performed an extensive literature review and adopted a pulse-based DC-IR characterisation method. By applying very short current pulses once the cell was fully relaxed, we were able to isolate the instantaneous voltage drop ($\Delta V = R \Delta I$) and derive accurate internal resistance values. Although the method required precise timing control and offered limited repetitive consistency, it enabled reliable DC-IR estimation throughout the test campaign, meeting the voltage resolution requirements and confirming internal stability across all cycles.

The SLPBB042126 cell was cycled 50 times from 3.0 V to 4.2 V and back, following the procedure defined in the technical report. The current profile replicated real braking behaviour on track ~1 minute lap time with 6–7 heavy braking events spaced 6–9 seconds apart, by superimposing high-current charge pulses during cycling. Temperature was continuously monitored with NTC sensors and thermal imaging, and a relay-based hardware cut-off (controlled via a MOSFET driver on a custom circuit) ensured safety in case of over-temperature, allowing controlled exposure from ~45 °C up to 60 °C.

Document:Formula Student
Date: 04/12/2025
Rev: 01
Page 22 of 73

Final Report Formula Student

BCN  **eMOTORSPORT**

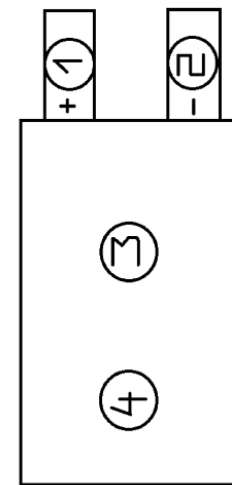
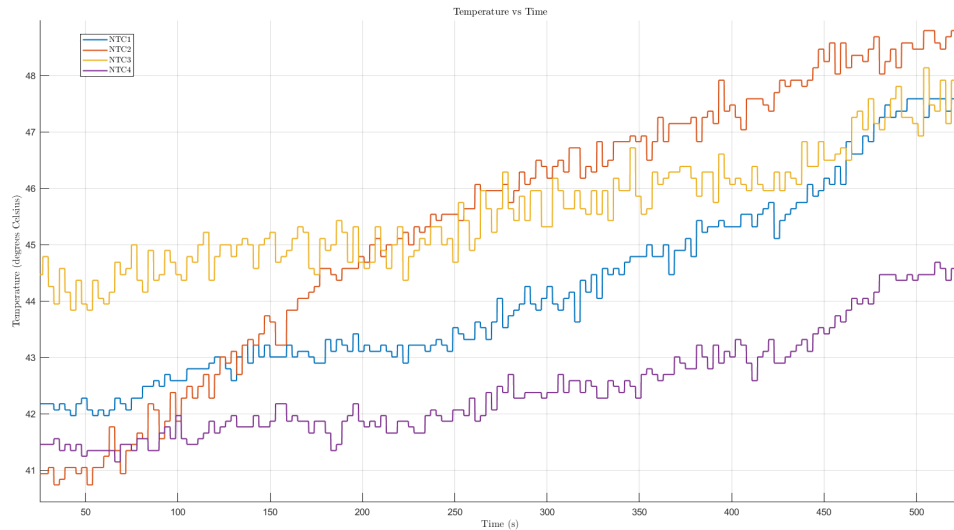
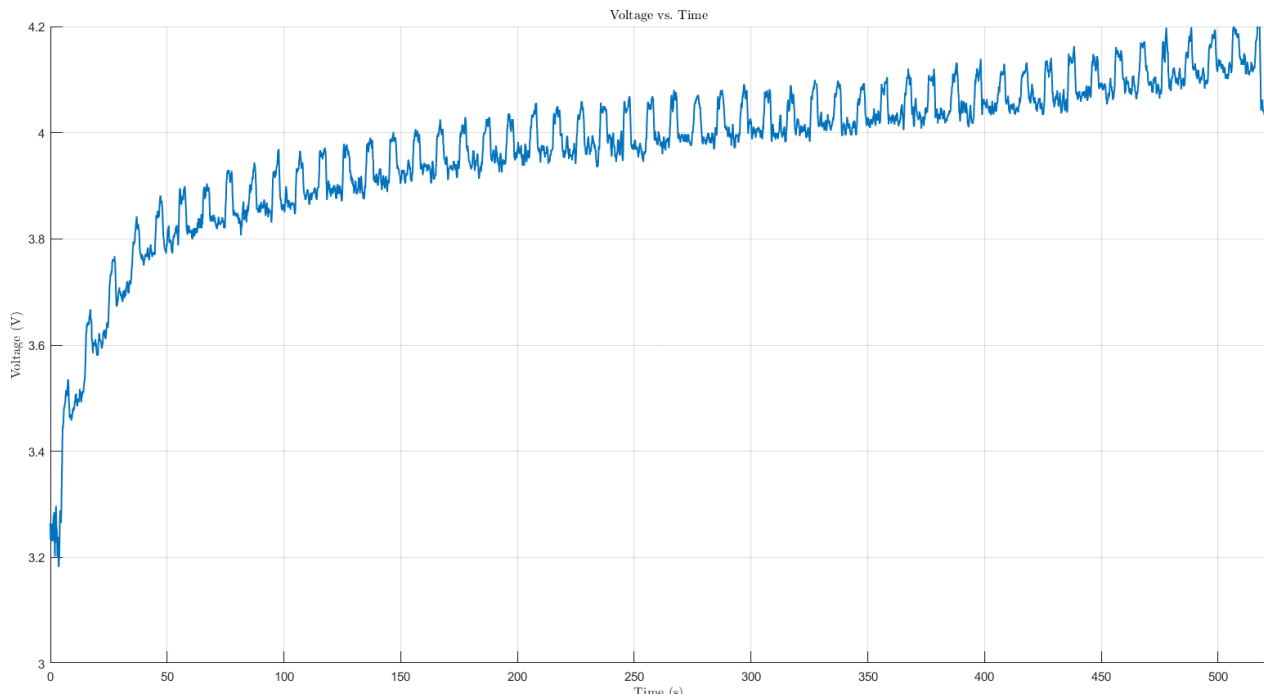


Image 10. Results of testing

Document:Formula Student	Final Report Formula Student	BCN eMOTORSPORT
Date: 04/12/2025		
Rev: 01		
Page 23 of 73		

Results showed stable impedance, no physical or thermal degradation, and negligible capacity loss, confirming that the SLPBB042126 cell can withstand the required regenerative current loads and thermal conditions for HV system integration. In consequence, a new datasheet was given by the manufacturer:

◆ 充电条件 Charge Condition	最大电流 Max. Continuous charge Current	13.2A	◆ 充电条件 Charge Condition	最大电流 Max. Continuous charge Current	27.4A	
	峰值充电 Peak charge current	19.8A($\leq 3\text{sec}$)		峰值充电 Peak charge current	50A($\leq 4\text{sec}$)	
	电压 Voltage	4.2V $\pm 0.03\text{V}$		电压 Voltage	4.2V $\pm 0.03\text{V}$	
◆ 放电条件 Discharge Condition	Max Continuous Discharge Current	99A	◆ 放电条件 Discharge Condition	Max Continuous Discharge Current	99A	
	Peak Discharge Current	148.5A($\leq 3\text{sec}$)		Peak Discharge Current	148.5A($\leq 3\text{sec}$)	
	Cut-off Voltage	3.0V		Cut-off Voltage	3.0V	
◆ 交流内阻 AC Impedance(mΩ)	≤ 2.0				◆ 交流内阻 AC Impedance(mΩ) ≤ 2.0	
◆ 循环寿命【充电:2C,放电:15C】 Cycle Life 【CHA:2C,DCH:15C】	$\geq 300\text{cycles}$				◆ 循环寿命【充电:2C,放电:15C】 Cycle Life 【CHA:2C,DCH:15C】 $\geq 300\text{cycles}$	
◆ 使用温度 Operating Temp.	充电 Charge	0°C~45°C	◆ 使用温度 Operating Temp.	充电 Charge	0°C~60°C	
	放电 Discharge	-20°C~60°C		放电 Discharge	-20°C~60°C	

Image 11. Information of datasheet

These cell test results directly translated into measurable performance gains on track. The improved current capability and higher regenerative acceptance allowed the vehicle to recover approximately 20% of the energy consumed per endurance lap, significantly reducing net energy expenditure and thermal stress on the HV battery system.

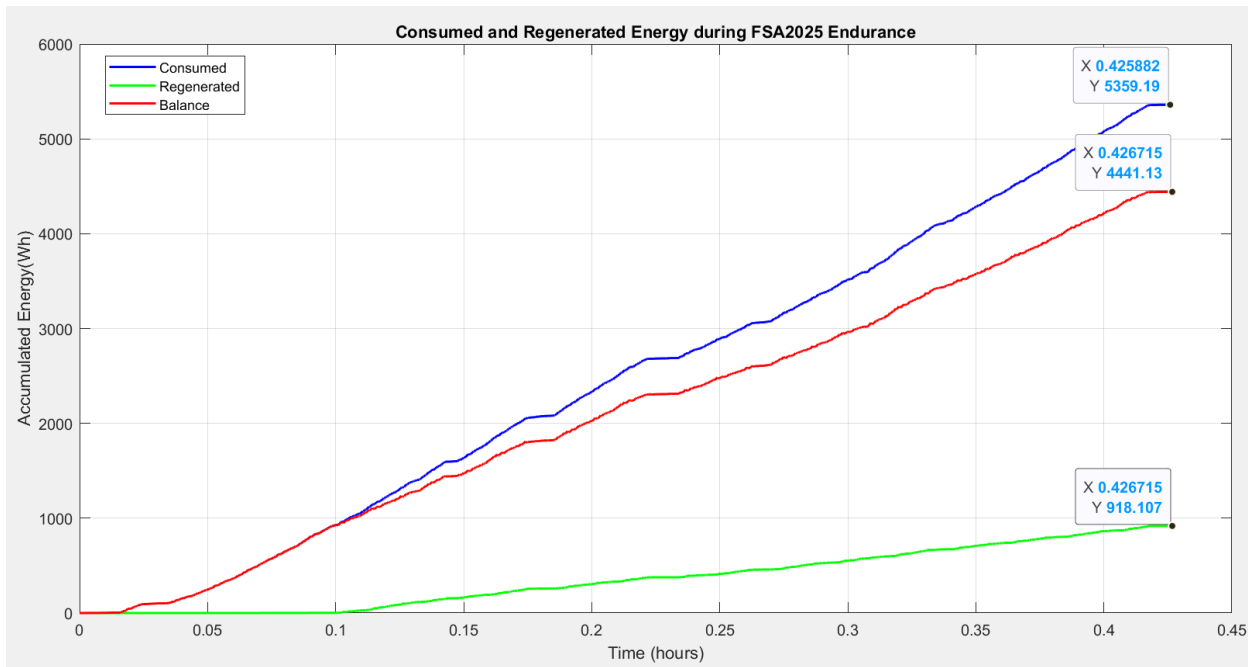


Image 12. Regenerated Energy during endurance

This improvement is reflected in the longitudinal velocity data: the CAT17x achieved an average of 9.16 m/s in the AutoX event, compared to 7.25 m/s for the CAT16x, clearly demonstrating the combined impact of improved energy efficiency, enhanced power delivery, and reduced voltage sag under load.

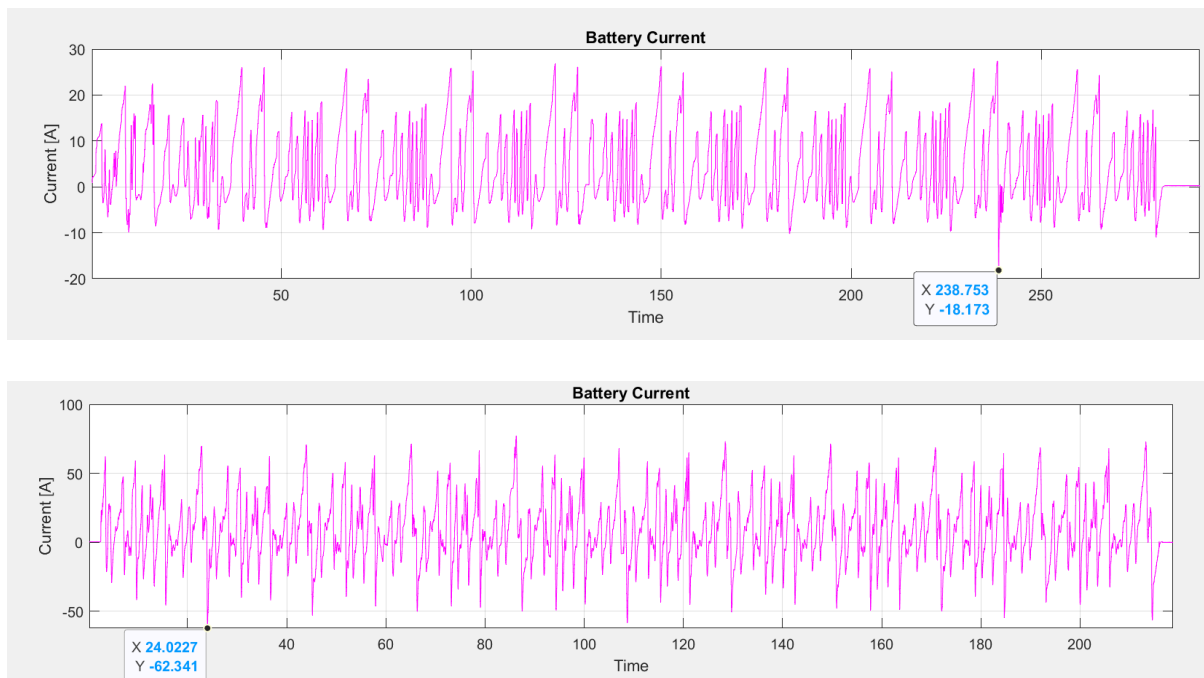


Image 13. Battery current

Document:Formula Student	Final Report Formula Student	BCN eMOTORSPORT
Date: 04/12/2025		
Rev: 01		
Page 25 of 73		

Overall, the validated cell behaviour enabled the system to operate closer to its optimal performance envelope, providing a decisive competitive advantage in both efficiency and lap-time capability.

BATTERY MODEL

The objective of the battery model was to create a reliable reference framework for future pack development and to build a deeper understanding of the behaviour of the cells used in the HV system. The model needed to predict voltage response under dynamic current profiles, estimate internal losses, and quantify polarisation effects across the state-of-charge range. These capabilities were required both for performance studies and for system-level design decisions, including cooling strategy, current limits, and regenerative operation.

To parameterise the model, Electrochemical Impedance Spectroscopy (EIS) measurements were carried out at the EEBE laboratory using a Gamry LPI1010 system. Two cells were tested at different states of charge to determine how impedance characteristics evolve with SOC. From the Nyquist plots, the parameters R_0 , R_1 , and C_1 were extracted and assigned to a first-order RC equivalent circuit structure. We performed EIS using a standard galvanostatic procedure with a four-wire configuration, applying a 65 mA AC excitation signal from 10 kHz down to 0.2 kHz, with all measurements carried out at 23 °C.



Image 14. Measurements

Due to limited lab time and only two available test cells, intermediate SOC values were interpolated and integrated into the model using lookup tables. The impedance results were processed using ZFit (EC-Lab) to obtain parameter estimates for each SOC point, allowing the model to reproduce measured dynamic response.

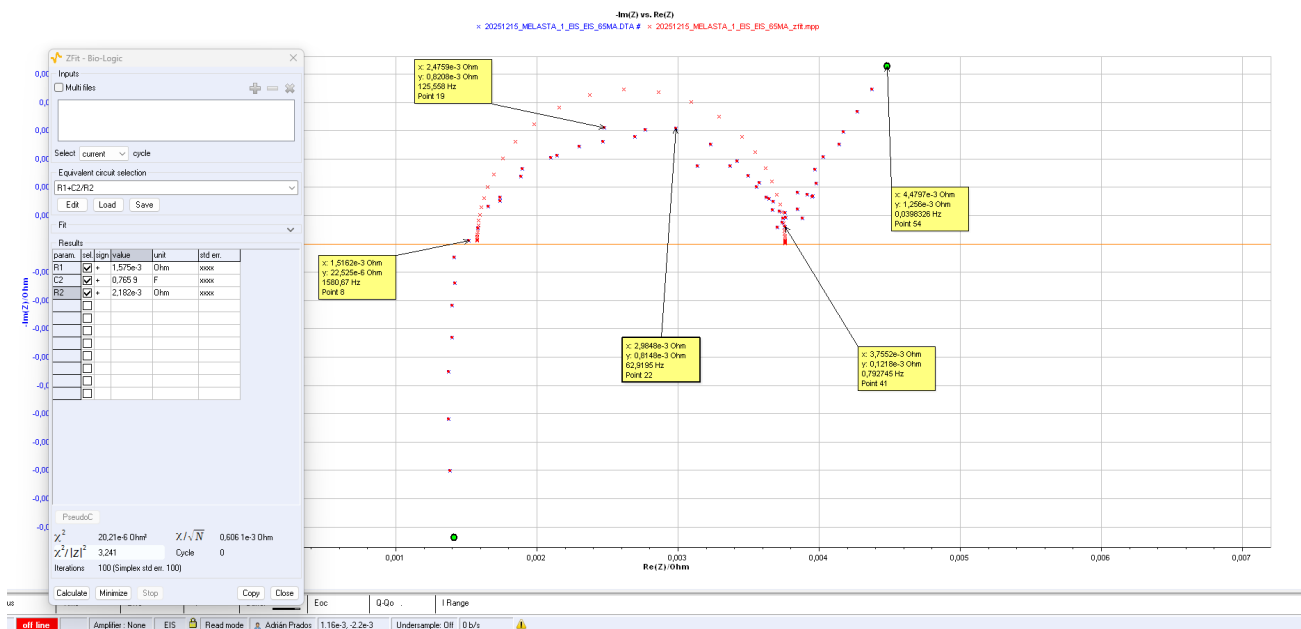
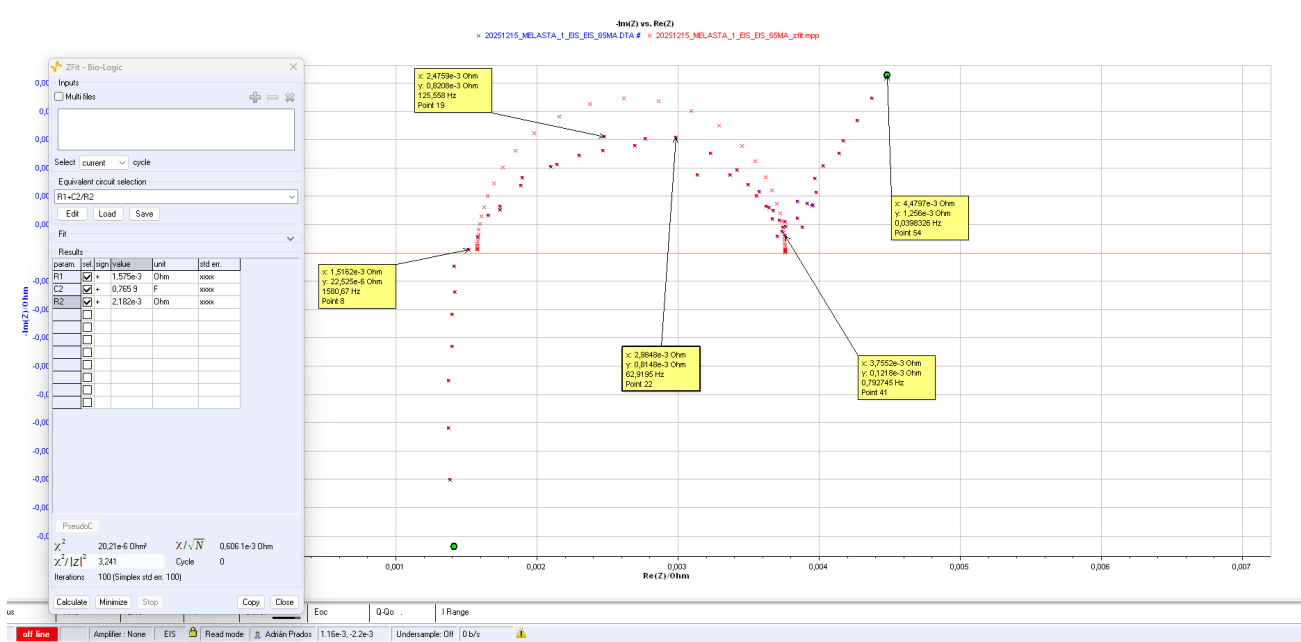


Image 15. Results of measurements

Document:Formula Student	Final Report Formula Student	
Date: 04/12/2025		
Rev: 01		
Page 27 of 73		

Voltage	SOC Estimation	R0(mΩ)	R1(mΩ)	C1 (F)
4.12 V	95%	1.575 m	2.182 m	0.7659
3.78 V	35%	1.575	2.741	0.8543

Table 2. Results

The increase in R_1 at lower SOC reflects higher charge-transfer resistance, meaning the electrochemical reaction becomes less efficient as available lithium decreases. The rise in C_1 indicates stronger capacitive (relaxation) effects, consistent with slower diffusion and higher polarisation. As a result, the RC time constant grows at lower SOC, leading to greater voltage drop during load changes, slower voltage recovery, and reduced power capability. This behaviour directly affects regenerative performance and current limits as SOC declines.

The mathematical model is based on three simple equations and Look up tables with the data gathered at testing.

Ohmic Drop due to DC resistances of the cell and the connection busbars:

$$\Delta V_0 = R_0 \cdot \Delta I$$

Polarisation branch that is in charge of

$$iR[k + 1] = e^{(-\frac{\Delta t}{R_1 C_1})} \cdot iR[k] + (1 - e^{(-\frac{\Delta t}{R_1 C_1})})i[k]$$

$$v[k] = OCV(z[k]) - R_0 \cdot i[k] - R_1 \cdot iR[k]$$

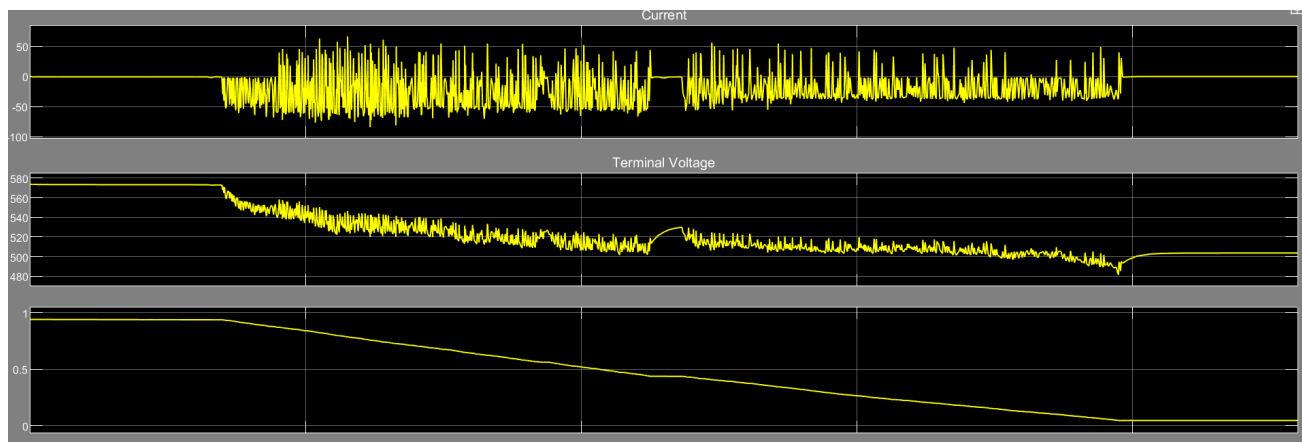
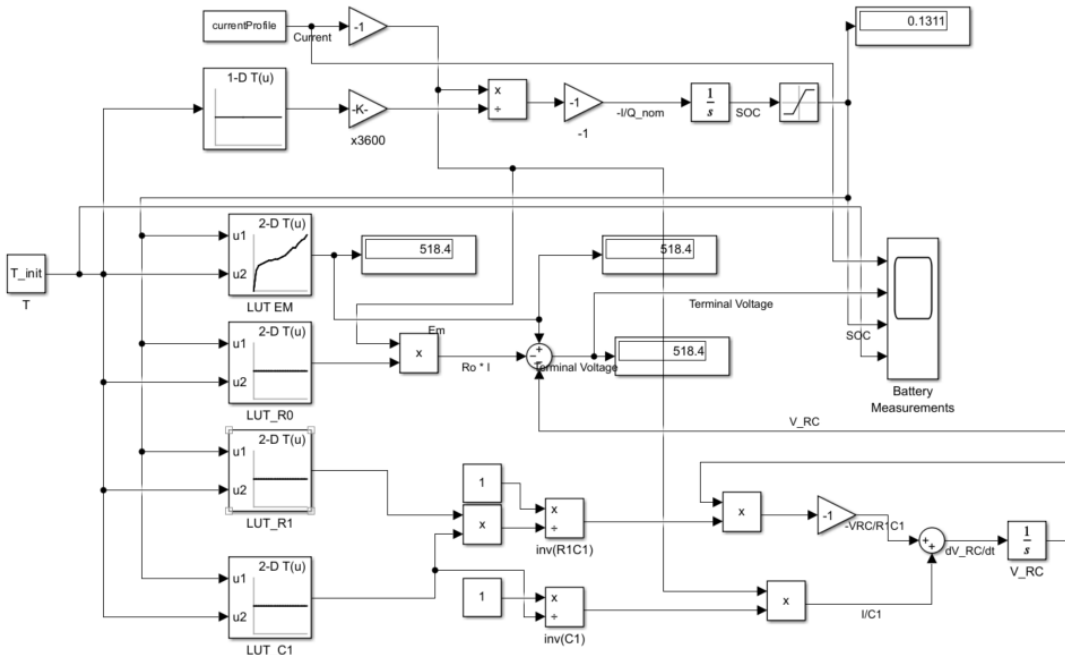


Image 16. Simulink analysis

For the applied current profile corresponding to the Formula Student Germany Endurance event, the simulation predicts a final state of charge of approximately 9%. In the real vehicle, the measured SOC at the end of the run was around 5%. This discrepancy is mainly attributed to higher ohmic losses in the real battery pack, including internal cell resistance, busbar losses, contact resistances, and cable losses, which are not fully captured in the simplified model. Despite this offset, the overall discharge behavior and energy consumption are well reproduced, indicating that the model provides a reliable and sufficiently accurate representation of the system.

Future work includes extending the parameter map to account for temperature dependence and ageing effects. In addition, diffusion resistance observed in the results could be incorporated into the model to enable a higher-order representation of cell dynamics. Once the battery pack is assembled, direct cell extraction is not feasible; however, combining field data with adaptive estimation methods and control modelling could allow parameters to be progressively updated during operation.